Supercapacitor Electrodes from Activated Carbon Monoliths and Carbon Nanotubes

2013 J. Phys.: Conf. Ser. 431 012015

(http://iopscience.iop.org/1742-6596/431/1/012015)

Supercapacitor Electrodes from Activated Carbon Monoliths and Carbon Nanotubes

B N M Dolah[1], M A R Othman[1,*], M Deraman[1], N H Basri[1], R Farma[1,2], I A Talib[1] and M M Ishak[1]

[1] School of Applied Physics, Faculty of Science and Technology, Universiti Kebangsaan Malaysia, 43600 Bangi, Selangor, Malaysia
[2] Department of Physics, Faculty of Mathematics and Natural Sciences, University of Riau, 28293 Pekanbaru, Riau, Indonesia

E-mail: maro@ukm.my

Abstract. Binderless monoliths of supercapacitor electrodes were prepared by the carbonization (N_2) and activation (CO_2) of green monoliths (GMs). GMs were made from mixtures of self-adhesive carbon grains (SACG) of fibers from oil palm empty fruit bunches and a combination of 5 & 6% KOH and 0, 5 & 6% carbon nanotubes (CNTs) by weight. The electrodes from GMs containing CNTs were found to have lower specific BET surface area (S_{BET}). The electrochemical behavior of the supercapacitor fabricated using the prepared electrodes were investigated by electrochemical impedance spectroscopy (EIS) and galvanostatic charge-discharge (GCD). In general an addition of CNTs into the GMs reduces the equivalent series resistance (ESR) value of the cells. A cell fabricated using electrodes from GM with 5% CNT and 5% KOH was found to have the largest reduction of ESR value than that from the others GMs containing CNT. The cell has steeper Warburg's slope than that from its respective non-CNT GM, which reflect the smaller resistance for electrolyte ions to move into pores of electrodes despite these electrodes having largest reduction in specific BET surface area. The cell also has the smallest reduction of specific capacitance (C_{sp}) and maintains the specific power range despite a reduction in the specific energy range due to the CNT addition.

1. Introduction

Supercapacitor, ultracapacitor or electrochemical double layer capacitor (EDLC) are the terms used to a class of electrical components that bridge the gap between capacitors and batteries. These components have unique characteristics for higher energy storage than conventional capacitor and faster in charging and discharging than batteries, which make them promising candidate for power application. Despite this, there are two areas where the performance of the supercapacitor can be further improved; their specific energy is lower than batteries and their specific power is lower than conventional capacitor.

A supercapacitor stores their energy through the formation of EDLC from electrostatic attraction, pseudocapacitance from quick faradaic charge transfer reaction and combination of both EDLC and pseudocapacitance effect. The EDLC which form from electrolyte ion's charge separation at the solution/electrode interfaces depends strongly on the electrodes surface area. The electrodes with high porosity have large specific surface areas which can promote the EDLC formation. One of the

prevailing sources of high porosity carbons is from biomass material because they are cheap and easily available in large quantities [1-11]. Some of these biomass material can be pre-carbonized to produce self-adhesive carbon grain (SACG) that can be converted into GMs form without the addition of any binding material [9, 12, 13]. These GMs have been converted into activated carbon pellet for application as electrode in supercapacitor [10, 11, 14]. However the electronic conductivity of activated carbon is low; in order of 10 to 100 S/m [15].

The electrical conductivity of the electrodes can be improved with the addition of CNTs into the green monoliths prior to electrode preparation because CNTs have a high electrical conductivity [16-18] in order of 10^3 (multi walled CNT [19]) to 10^8 (single walled CNT [20]) S/m. The purpose of adding the CNTs in the electrodes is to decrease the equivalent series resistance of the supercapacitor cells so that the specific power of the cells will be improved [21].

In the present study, the supercapacitor cells whose electrodes were prepared from three batches of mixtures with different combination of SACG, KOH and CNTs percentages were investigated by electrochemical impedance spectroscopy (EIS) and galvanostatic charge-discharge (GCD). The objective of this study is to determine their electrochemical behaviors, focusing on the correlation between the change in electrode porosity with specific capacitance, specific power, specific energy and ESR of the cells resulted from the present of CNTs in the electrodes.

2. Experimental details

2.1. Sample preparation

The activated carbon monoliths (ACMs) were prepared from fibers of empty fruit bunch (EFB) precursor by employing our previously reported method [22]. The EFB was first pre-carbonized (Furnace CTMSB46) at temperature of ~280 ^{o}C, followed by ball-milling process (ball-mill AC Motor BS 500-110) for 36 hours and sieving (Matest 24030 Brembate Sopra (BG)) to obtain SACG of particle size less than 106 microns. The composition for the mixtures of SACG, KOH, and CNTs, based on the weight percentages shown in table 1, were prepared and then converted into GMs using a press pelletizing machine (VISITEC 2009-Malaysia) with 8 tonnes of compressive force inside a mold (20 mm in diameter). Justification for selecting the composition shown in Table 1 was based on the results reported in reference [9].

Carbon monoliths (CMs) were then produced from GMs via carbonization process (Vulcan Box Furnace 3-1750) that was done separately according to their batches under N_2 gas with flow rate of 1.5 *l*/min [22, 23]. ACMs production were then continued with CO_2 activation (1 *l*/min flow rate) of the CMs at temperature of ~800 ^{o}C with 3 hour holding time [22]. The ACMs were polished to a desired thickness and washed with distilled water to achieve pH 7. The ACMs were used in symmetrical supercapacitor cells as electrodes with 0.4 mm in thickness. The cells were assembled using stainless steel 316L as current collector, 1 M sulfuric acid (H_2SO_4) as electrolyte, Teflon ring as a separator (0.1 mm) and cured resin as a housing. The cells fabricated were labeled according to the codes shown in table 1.

2.2. Physical and electrochemical characterizations

Measurement for the dimensions (Mitutoyo 193-253) and weight (Mettler Toledo AB204) of GMs, CMs, and ACMs produced from each batch were taken to determine the sample density. Studies on the microstructure of the electrodes fractured surface were carried out using Field Emission Scanning Electron Microscopy (FESEM) (Ziess SUPRA 55VP). The porosity properties of the ACMs were characterized using nitrogen adsorption-desorption isotherm technique (ASAP 2010, Micromeritics) at 77 K. The data collected from this technique were used to calculate the specific surface area (S_{BET}), micropore surface area (S_{micro}), mesopore surface area (S_{meso}), micropore volume (V_{micro}), mesopore volume (V_{meso}), total pore volume (V_{total}) and average pore diameter (D_p) of the ACMs by using the standard methods [24, 25].

Table 1. Composition of green, carbon and activated carbon monoliths and their labels.

Batch-Type	Green Monolith (% by weight)				Carbon Monolith	Activated Carbon Monolith
	SACG	KOH	CNT	Label		
1-1	95	5	0	GM1150	CM1150	ACM1150
1-2	90	5	5	GM1255	CM1255	ACM1255
2-1	95	5	0	GM2150	CM2150	ACM2150
2-3	89	5	6	GM2356	CM2356	ACM2356
3-4	94	6	0	GM3460	CM3460	ACM3460
3-5	89	6	5	GM3565	CM3565	ACM3565

Table 2. Weight and dimension of ACMs.

ACMs	Weight (g)	Tickness (mm)	Diameter (mm)	Density (g/cm^3)
ACM1150	0.26	1.49	14.13	1.13
ACM1255	0.29	1.56	14.92	1.07
ACM2150	0.30	1.91	14.67	0.93
ACM2356	0.33	2.02	15.53	0.86
ACM3460	0.32	1.69	14.55	1.14
ACM3565	0.33	1.78	15.27	1.01

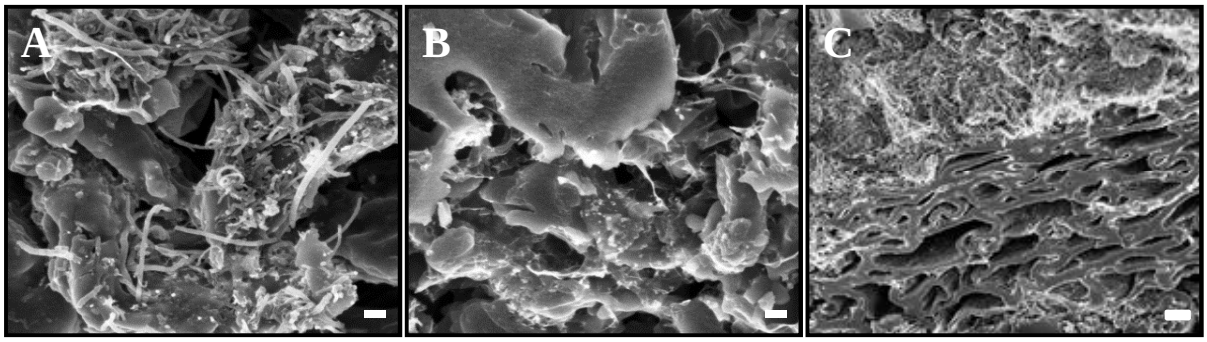

Figure 1. FESEM images of the fractured surface of (a) the ACM1150 with 20,000× magnifications and ACM1255 electrodes with (b) 20,000× and (c) 2,500× magnifications.

The electrochemical behavior of the supercapacitor cells fabricated was characterized by EIS and GCD (Solartron 1287). All the measurements were conducted at room temperature (25 ^{o}C). The EIS measurement was conducted over a frequency range of 500 kHz to 10 mHz, and the GCD measurement was conducted at a current density of 10 mA cm^{-2}.

3. Results and discussion

The weight and dimension of ACMs from SACG mixed with varying combination of KOH and CNT are shown in table 2. This table shows that the addition of CNTs reduced the density of the ACMs.

The porous properties of the samples with and without CNTs are clearly revealed by the presence of macropores in the FESEM images recorded at 20,000 and 2,500 magnification scales in figure 1. The shape, orientation and distribution of the ACMs grains look very similar for both samples, ACM1150 and ACM1255, in figures 1(a) and 1(b) respectively. The present of CNTs can be seen in the figure 1(b); there are unoccupied mesopores and macropores occupied by CNTs which are in agglomerated form. However, at low magnification of 2,500×, it is revealed that the CNTs is mostly occupied the outer pores and the pores within the grains remains unoccupied. This type of CNTs distribution creates spacing between grains where it lowers the electrodes density as in table 2.

It was found that the nitrogen adsorption-desorption isotherm data exhibited a typical type IV isotherm curve for all the ACMs samples. Figure 2 shows the comparisons of nitrogen absorption-desorption capacities for all batches. It indicates that ACMs from all batches were porous, consisting both meso and micro pores; with a high internal surface area. However the electrodes with CNTs have lower absorption-desorption capacities compared to electrodes without CNTs. Table 3 list the porosity parameter values obtained from the nitrogen absorption-desorption data. Generally, the additions of CNTs into the electrodes lower the S_{BET}. This behavior is shown by the value of S_{micro}, S_{meso}, V_{micro}, V_{meso} (except for Batch 3) and D_p for electrodes with and without CNTs as in Table 3. ACM1255 has the largest reduction of S_{BET}, S_{micro} and S_{meso} compared to the electrodes without CNTs (ACM1150). This is in agreement with other study that show decrease in S_{BET} when CNTs was added into activated carbon derived from seaweed [26]. The CNTs have very small specific surface area of about 82 m^2/g [27] but very high conductivity. Thus, by mixing small portion of CNTs into active material with high specific surface area, the good conductivity of CNTs can be inherited by the new composite.

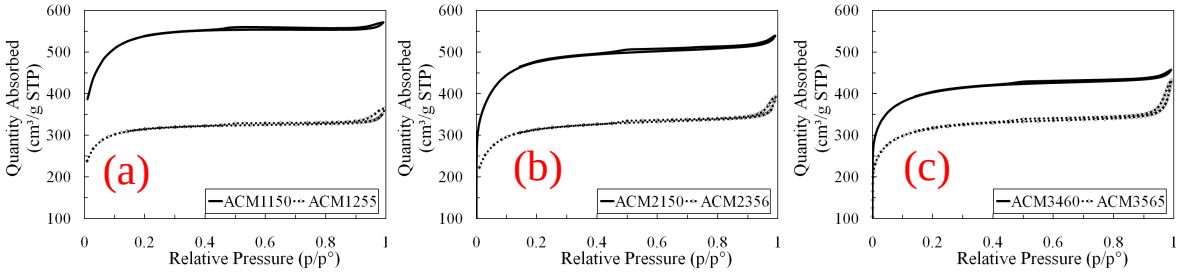

Figure 2. Nitrogen adsorption-desorption isotherm for Batches 1 (a), 2 (b) and 3 (c).

Table 3. The values of ACMs porosity parameters.

ACMs	Porosity Parameters					
	S_{BET} (m^2/g)	S_{meso} (m^2/g)	S_{micro} (m^2/g)	V_{meso} (cm^3/g)	V_{micro} (cm^3/g)	D_p (nm)
1150	1704	539	1165	0.16	0.62	2.1
1255	987	279	708	0.13	0.38	2.2
2150	1592	656	936	0.31	0.45	2.1
2356	1001	395	606	0.20	0.33	2.4
3460	1349	495	855	0.24	0.41	2.1
3565	1056	343	713	0.31	0.34	2.4

The EDLC behavior is associated with the diffusion of electrolyte ions into pores of the porous electrodes. Thus its diffusion depends on many factors such as electrolyte resistance, current collector intrinsic resistance, active material/electrolyte interface resistance, active material intrinsic resistance and contact resistance between particles [18]. The electrochemical behavior of the samples was determined from the EIS and GCD measurements.

The EIS data presented in a form of the Z" versus Z' is known as a Nyquist plot. A typical Nyquist plots for EDLC behavior consisting three significant part of a semi-circle curve at high frequency region, a Warburg line (slope ~ 45°) at intermediate frequency region and a nearly straight vertical line at low frequency region. This typical plot can be seen in figure 3, i.e. for the samples with and without CNTs, ACM1255 and ACM1150, respectively. The Nyquist plots of EIS data for the other batches show a very similar shape of Nyquist plot (not shown here). These data show that the cells using electrode with and without CNTs exhibit EDLC behavior. The diameter of the semi-circle curve represents the ESR of the cells, as shown in the inset of figure 3, which depends on the pore characteristic of the ACMs and ionic accessibility into the ACM's pores [28]. The Warburg's slope in

the EIS represents ion diffusion resistance in the porous electrodes. The slope's 45° angle represent *-j* gradient in Nyquist plot. The low frequency region represents the cells capacitance dominant region.

The ESR values are lower for electrodes with CNTs as shown in figure 4. The largest decrease in ESR value was for ACM1255. The decrease in ESR for electrodes with CNTs can be attributed to the uniform network of highly conductive CNTs that effectively lower the active material intrinsic resistance and contact resistance between particles. This increases the polarization range in the electrodes far from the current collector metal. This is trivial in a 0.4 mm-thick electrode.

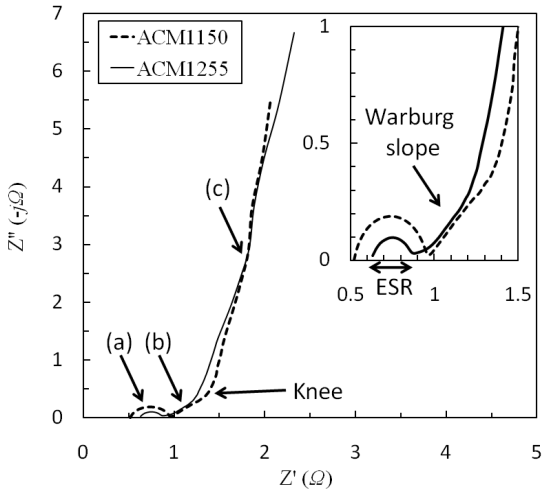

Figure 3. The ESR, Warburg slope and knee in Nyquist plot for ACM1150 and ACM1255. Shown are (a) the semi-circle curves at high frequency regions, (b) Warburg lines (slope ~45°) at intermediate frequency regions and (c) nearly straight vertical lines at low frequency regions.

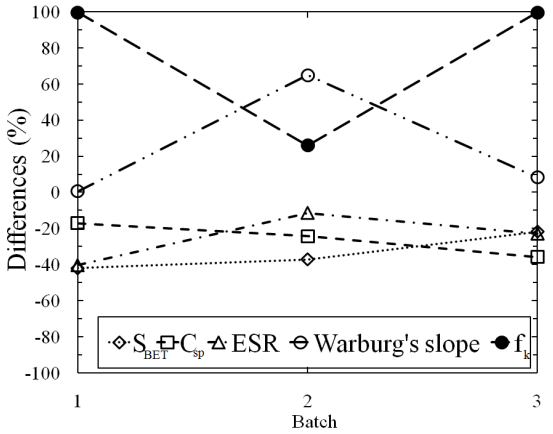

Figure 4. The differences of EIS parameters in percentage for electrodes with CNTs compared to electrodes without CNTs for all batches.

Figure 4 show that ACM2356 has the highest increase in the Warburg's slope gradient, indicating the effect of CNTs in the sample. Whereas there are almost no changes in the other two ACMs batches. The specific capacitance was calculated from the EIS data using $C_{sp} = -2/(2\pi m f|Z''|)$, where m is the mass of one electrode, f is the frequency and $|Z''|$ is the magnitude of imaginary impedance. C_{sp} at f = 10 mHz was found to decrease with the addition of CNTs. The smallest reduction of C_{sp} was from ACM1255 (-17 %) even though S_{BET} was reduced (-42 %) as shown in figure 4. This prove that the gain or reduction in C_{sp} is not a linearly proportional with S_{BET} but depends on the effectiveness of double layer formation [29]. Knee in the Nyquist plot is a point that joints the Warburg line and the nearly vertical line of capacitance dominant region at low frequency as in figure 3. Thus, a knee frequency, f_k, is a maximum frequency where the capacitive behavior is dominant. The higher f_k gained by electrodes containing CNTs as shown in figure 4 depict an improvement in their specific power [30]. However higher f_k shift the lowest frequency point (10 mHz) to higher impedance value (|Z|), which result decrease in C_{sp} of the electrodes.

Figure 5 shows a comparison of the GCD behavior of all batches over a potential range of 0–1 V and a current density of 10 mA cm^{-2}. Both the charge and discharge curves of all batches exhibit an almost linear behavior; a typical shape for carbon based supercapacitors. Both cells show a sharp voltage drop at the beginning of the discharge curves, which is associated with the ESR of the supercapacitor cells. The cells with CNTs charged and discharged quicker than the cells without CNTs as shown by smaller duration needed to perform the charge-discharge cycle, however due to they have smaller areas under the charge-discharge curve reflect their smaller capacitance values.

The values of the specific power (P) and specific energy (E) were calculated from the charge–discharge curves (figure 5) using the equations $P = Vi/m$ and $E = Vit/m$, respectively, where i is the discharge current, V is the voltage excluding the iR drop occurring at the beginning of the discharge, t is time and m is the mass [28]. Figure 6 shows Ragone plots that compared the variation of the P with the E of the cells with and without CNTs. All cells show a typical specific power-energy relationship and exhibit a very similar shape, with a specific energy that remains almost unchanged at low specific power and then gradually decreases before showing a relatively larger decrease in the region of higher

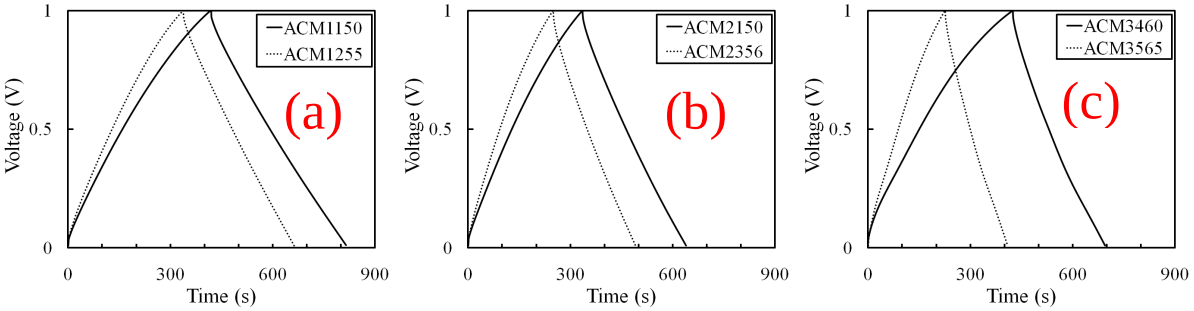

Figure 5.Charge–discharge curves for Batch 1 (a), Batch 2 (b) and Batch 3 (c), measured for current density at 10 mA cm^{-2}.

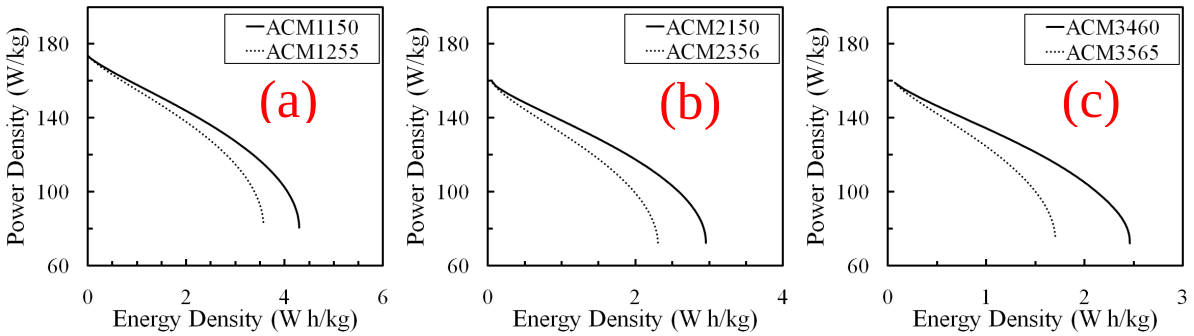

Figure 6. Ragone plots of specific power-energy correlations, for Batch 1 (a), Batch 2 (b) and Batch 3 (c).

specific power. Although the results show a very similar shape, the differences in their values clearly indicates the role of CNTs in improving specific power-energy relationship, with a maximum specific energy of 3.6 Wh kg^{-1} corresponding to a specific power of 82 W kg^{-1} over the electrodes without CNTs.

4. Conclusion

The supercapacitor cells fabricated from electrodes prepared by chemical and physical activation of GMs containing pre-carbonized biomass and mixtures of pre-carbonized biomass and small portion of CNTs, respectively, were investigated. It was found that the addition of small quantity (5 – 6 % by weight) of CNTs reduced the specific surface area and specific capacitance of the electrodes, but it can improve electronic conductivity of electrodes as revealed by the decrease in the ESR values of the cells. This improvement is associated with results that the cells with CNTs have smaller specific energy range but can retain their specific power range.

Acknowledgments

We acknowledged the grants from the Universiti Kebangsaan Malaysia (UKM-GUP-216-2011, UKM-DLP-2012-022, UKM-DLP-2012-023), and the support of CRIM (Centre for Research and Innovation Management). The author also thank to Mr. Saini Sain for helping with the laboratory work.

References

[1] Ismanto A E, Wang S, Soetaredjo F E and Ismadji S 2010 *Bioresource Technol.* **101** 3534-40
[2] Jisha M R, Hwang Y J, Shin J S, Nahm K S, Prem Kumar T, Karthikeyan K, Dhanikaivelu N, Kalpana D, Renganathan N G and Stephan A M 2009 *Mater. Chem. Phys.* **115** 33-9
[3] Liu L, Liu Z, Huang Z, Liu Z and Liu P 2006 *Carbon* **44** 1598-601
[4] Olivares-Marín M, Fernández J A, Lázaro M J, Fernández-González C, Macías-García A, Gómez-Serrano V, Stoeckli F and Centeno T A 2009 *Mater. Chem. Phys.* **114** 323-7
[5] Rufford T E, Hulicova-Jurcakova D, Khosla K, Zhu Z and Lu G Q 2010 *J. Power Sources* **195** 912-8
[6] Rufford T E, Hulicova-Jurcakova D, Zhu Z and Lu G Q 2008 *Electrochem. Commun.* **10** 1594-7
[7] Subramanian V, Luo C, Stephan A M, Nahm K S, Thomas S and Wei B 2007 *J. Phys. Chem. C* **111** 7527-31
[8] Wu F C, Tseng R L, Hu C C and Wang C C 2006 *J. Power Sources* **159** 1532-42
[9] Deraman M, Saad S K M, Ishak M M, Awitdrus, Taer E, Talib I A, Omar R and Jumali M H 2010 *AIP Conf. Proc.* **1284** 179-86
[10] Taer E, Deraman M, Talib I A, Umar A A, Oyama M and Yunus R M 2010 *Curr. Appl. Phys.* **10** 1071-5
[11] Taer E, Deraman M, Talib I A, Awitdrus, Hashmi S A and Umar A A 2011 *Int. J. Electrochem. Sc.* **6** 3301-15
[12] Deraman M, *et al.* 2010 *AIP Conf. Proc.* **1325** 50-4
[13] Awitdrus, Deraman M, Talib I A, Omar R, Jumali M H H, Taer E and Saman M M 2010 *Sains Malays.* **39** 83-6
[14] Awitdrus, Deraman M, Talib I A, Farma R, Omar R and Ishak M M 2012 *Adv. Mat. Res.* **501** 13-8
[15] El-Kady M F, Strong V, Dubin S and Kaner R B 2012 *Science* **335** 1326-30
[16] Deraman M, Ishak M M, Farma R, Awitdrus, Taer E, Talib I A and Omar R 2011 *AIP Conf. Proc.* **1415** 175-9
[17] Farma R, Deraman M, Omar R, Awitdrus, Ishak M M, Taer E and Talib I A 2011 *AIP Conf. Proc.* **1415** 180-4
[18] Portet C, Taberna P L, Simon P and Flahaut E 2005 *J. Power Sources* **139** 371-8
[19] Pham G T, Park Y B, Liang Z, Zhang C and Wang B 2008 *Compos. Part B-Eng.* **39** 209-16
[20] Yang Y L, Wang Y D, Ren Y, He C S, Deng J N, Nan J, Chen J G and Zuo L 2008 *Mater. Lett.* **62** 47-50
[21] Kötz R, Hahn M and Gallay R 2006 *J. Power Sources* **154** 550-5
[22] Deraman M, Omar R, Zakaria S, Mustapa I R, Talib M, Alias N and Jaafar R 2002 *J. Mater. Sci.* **37** 3329-35
[23] Deraman M, Omar R, Harun A G and Ismail M P 1998 *Journal of Materials Science Letters* **17** 2059-60
[24] Brunauer S, Emmett P H and Teller E 1938 *J. Am. Chem. Soc.* **60** 309-19
[25] McEnaney B 1987 *Carbon* **25** 69-75
[26] Raymundo-Piñero E, Cadek M, Wachtler M and Béguin F 2011 *Chemsuschem* **4** 943-9
[27] Lu W, Hartman R, Qu L and Dai L 2011 *J. Phy. Chem. Lett.* **2** 655-60
[28] Taer E, Deraman M, Talib I A, Hashmi S A and Umar A A 2011 *Electrochim. Acta* **56** 10217-22
[29] Obreja V V N 2008 *Physica E* **40** 2596-605
[30] Du C and Pan N 2006 *Nanothechnology* **17** 5314-8